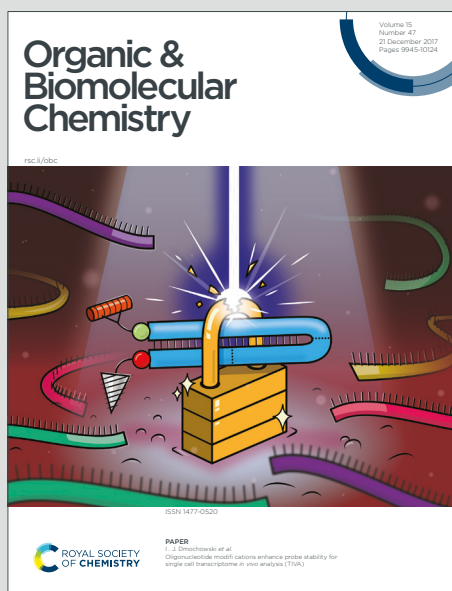


Organic & Biomolecular Chemistry

Accepted Manuscript

This article can be cited before page numbers have been issued, to do this please use: C. Gimbert Suriñach, R. Pleixats, A. Granados and A. Vallribera, *Org. Biomol. Chem.*, 2025, DOI: 10.1039/D6OB00441E.



This is an Accepted Manuscript, which has been through the Royal Society of Chemistry peer review process and has been accepted for publication.

Accepted Manuscripts are published online shortly after acceptance, before technical editing, formatting and proof reading. Using this free service, authors can make their results available to the community, in citable form, before we publish the edited article. We will replace this Accepted Manuscript with the edited and formatted Advance Article as soon as it is available.

You can find more information about Accepted Manuscripts in the [Information for Authors](#).

Please note that technical editing may introduce minor changes to the text and/or graphics, which may alter content. The journal's standard [Terms & Conditions](#) and the [Ethical guidelines](#) still apply. In no event shall the Royal Society of Chemistry be held responsible for any errors or omissions in this Accepted Manuscript or any consequences arising from the use of any information it contains.

ARTICLE

Light mediated asymmetric approaches towards alkene difunctionalization

Carolina Gimbert-Suriñach, Roser Pleixats, Albert Granados,* Adelina Vallribera*

Received 00th January 20xx,
Accepted 00th January 20xx

DOI: 10.1039/x0xx00000x

Visible-light photochemistry has emerged as a powerful platform for the development of asymmetric radical transformations under mild and sustainable conditions. Particularly, the enantioselective difunctionalization of alkenes enables the rapid construction of molecular complexity through the simultaneous formation of two bonds across the C=C bond, providing rapid access to highly functionalized optically active organic skeletons. Despite the remarkable progress achieved in racemic variants, asymmetric light-driven processes remain comparatively underexplored due to the challenges associated with stereocontrol in open-shell pathways. This review highlights recent advances in light-mediated asymmetric alkene difunctionalization, with particular emphasis on the strategies that enable efficient enantiocontrol. The discussion is organized according to the mode of stereochemical induction, including metallaphotoredox dual catalysis, cooperative photoredox catalysis combined with chiral hydrogen-bonding catalysts, and the use of enantioenriched reagents as traceless chiral auxiliaries. Special attention is given to mechanistic features that govern radical generation, metal-radical interception and enantiodetermining bond-forming scenarios. By providing a unified overview of these complementary approaches, this review outlines the current state of the art and future opportunities for the development of general, efficient and sustainable asymmetric multicomponent reactions driven by visible light.

Introduction

Alkenes are abundant, readily available feedstocks and constitute one of the most privileged and versatile functional groups in organic synthesis, being prone to both electrophilic and radical addition processes.¹ Consequently, they have emerged as ideal platforms for the rapid construction of molecular complexity. In this context, the difunctionalization of alkenes has become a powerful synthetic strategy, enabling the simultaneous installation of two different functional groups across the π -system and thus allowing the formation of C–C and C–X bonds in a single operation.² Although numerous 1,2-difunctionalization methods have been developed,³ asymmetric variants remain comparatively less exploited.⁴ Representative examples include photoredox/nickel-catalyzed aminoalkylation processes and radical-relayed reductive couplings that provide enantioenriched products from simple precursors.

Visible-light photoredox catalysis has revolutionized radical chemistry by enabling mild generation of reactive intermediates with high functional-group tolerance.⁵ This activation mode offers a promising platform for multicomponent stereoselective transformations.⁶ In addition, photoelectrocatalysis⁷ expands the accessible redox window, allowing oxidative processes under milder conditions.

Excellent extensive reviews have been published until now including a general review on the intermolecular 1,2-

difunctionalization of alkenes.^{2a,8} Herein, we focus on the most recent advances in the asymmetric 1,2-difunctionalization of alkenes under light-mediated conditions. The discussion is organized according to the different stereocontrol strategies, metallaphotoredox dual catalysis, cooperative chiral hydrogen-bonding/photoredox catalysis and the use of chiral reagents.

Metallaphotoredox dual catalysis

Metallaphotoredox catalysis merges a photoredox catalytic cycle with a transition-metal cross-coupling cycle. Photoexcitation of the photocatalyst enables the generation of radical intermediates that are intercepted by metal complexes, typically operating through $\text{Ni}^0/\text{Ni}^{\text{I}}/\text{Ni}^{\text{III}}$ or $\text{Cu}^{\text{I}}/\text{Cu}^{\text{II}}/\text{Cu}^{\text{III}}$ manifolds. Reductive elimination from high-valent intermediates generally delivers the stereocontrolled product, with enantioinduction dictated by a coordinated chiral ligand.⁹ This section is divided into nickel, copper or chromium dual photoredox methods.

Dual nickel/photoredox catalytic systems

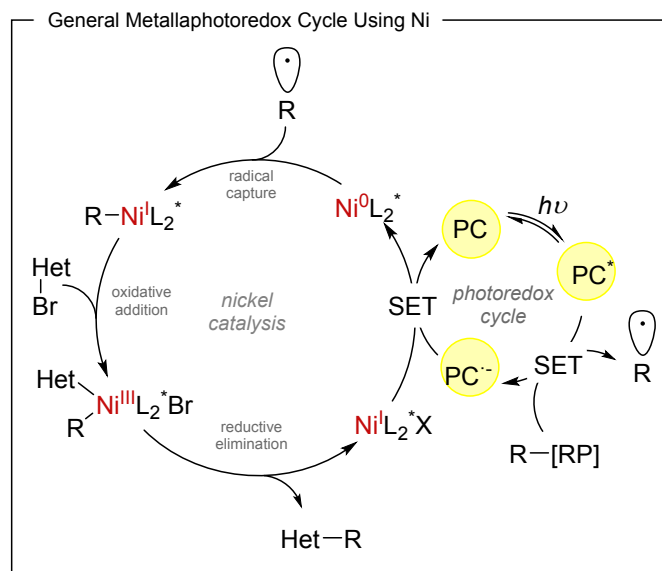
In recent years, nickel has emerged as a key metal in transition-metal catalysis and, in particular, in dual metallaphotoredox processes. Compared with palladium, nickel is more abundant and exhibits a higher propensity for oxidative addition into alkyl electrophiles, while also showing a lower tendency toward β -hydride elimination with aliphatic ligands. These features,

Departament de Química and Centro de Innovación en Química Avanzada (ORFEO-CINQA), Universitat Autònoma de Barcelona, Cerdanyola del Vallès, 08193 Barcelona, Spain. E-mail: albert.granados@uab.es, adelina.vallribera@uab.es



ARTICLE

Journal Name



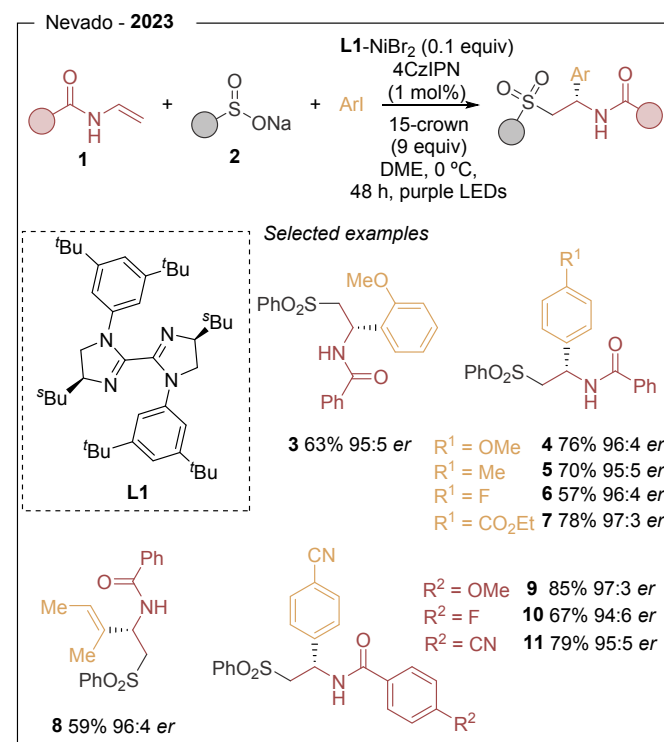
Scheme 1. General mechanism for the photoredox/Ni dual catalysis processes.

together with its ability to engage in single-electron processes, have enabled the rapid expansion of nickel catalysis in radical-based asymmetric transformations. The metallaphotoredox strategy relies on two interconnected catalytic cycles, a photoredox cycle and a nickel-catalysed cross-coupling cycle (Scheme 1). Upon visible-light irradiation, the photocatalyst (PC) is promoted to its excited state (PC*), which typically initiates the process through single-electron transfer (SET) with a radical precursor (RP-R), generating the corresponding open shell species (R·). In a reductive quenching manifold, the reduced form of the photocatalyst then closes the photoredox cycle by reducing the nickel intermediate, thereby enabling turnover of the metal catalytic cycle. A common mechanistic feature of these transformations is the involvement of Ni⁰/Ni^I/Ni^{III} species.¹⁰ The radical generated in the photoredox cycle is intercepted by a chiral Ni⁰ complex to form an R-Ni^I intermediate, which undergoes oxidative addition with an electrophile (Het-Br, for example) to furnish a high-valent Ni^{III} species. Reductive elimination from a L*(Het)(R)Ni^{III}X intermediate delivers the final product in a stereocontrolled manner and regenerates the Ni^I species. Enantioinduction in these reactions is achieved through the use of C₂-symmetric chiral ligands that remain coordinated to the nickel centre throughout the catalytic cycle. Among the different ligand families explored, chiral biimidazoline derivatives have consistently provided the highest levels of enantioselectivity in the transformations discussed in this review.

In 2023, Nevado¹¹ reported an asymmetric three-component carbonylsulfonylation of alkenes that enables the simultaneous formation of C-C and C-S bonds across the double bond. This visible-light-driven protocol provides enantioenriched β-aryl and β-alkenyl sulfones from vinylamides, aryl or alkenyl halides, and aryl sulfonates under the combined action of the organic photocatalyst 4CzIPN (1,2,3,5-tetrakis(carbazol-9-yl)-4,6-dicyanobenzene), NiBr₂ as catalyst and biimidazoline **L1** as chiral

ligand (Scheme 2). A wide range of vinylamides (**1**) and sulfonate salts (**2**)

DOI: 10.1039/D6OB00441E

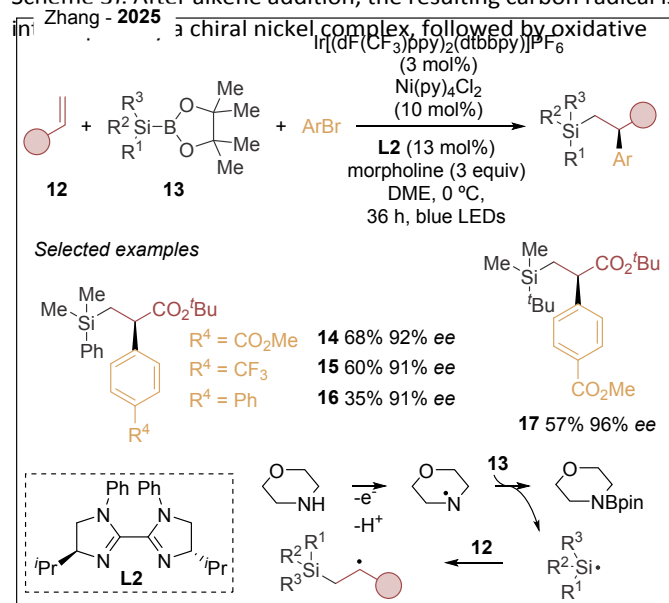


Scheme 2. Carbonylsulfonylation of vinylamides reported by Nevado and collaborators.

proved to be suitable reaction partners, and the method was applicable to the late-stage functionalization of complex molecules. Overall, 51 examples were reported with excellent levels of regio- and enantiocontrol, reaching enantiomeric ratios up to 99:1 *er* (**3-11**). Mechanistically, photoexcited 4CzIPN oxidizes the sulfonate to generate a sulfonyl radical, which adds to the alkene to form a secondary carbon-centered radical. This intermediate is captured by the chiral nickel complex, and subsequent oxidative addition and reductive elimination complete the stereocontrolled cross-coupling (see Scheme 1). Further diversification of this strategy was reported by Zhang in 2025 (Scheme 3).¹² The first light-induced asymmetric silylation of alkenes was described, enabling the simultaneous formation of C-C and C-Si bonds. This three-component protocol, based on terminal alkenes (**12**), aryl bromides and silylboranes (**13**), provides access to enantioenriched β-silyl-α-aryl propionates. Optimal results were obtained using the iridium photocatalyst Ir[(dF(CF₃))ppy]₂(dtbbpy)]PF₆ in combination with Ni(py)₄Cl₂ as the nickel source and **L2**. More than 30 compounds were accessed, demonstrating high chemoselectivity, excellent functional-group tolerance and outstanding enantiomeric excesses of up to 96% (**14-17**). The reaction generally proceeded in moderate yields, and electron-rich aryl bromides were less effective coupling partners, likely due to their slower oxidative addition to the nickel centre. The presence of 3 equiv of morpholine was found to be crucial for efficient reactivity. On the basis of mechanistic studies, photoexcited Ir oxidizes



morpholine, generating an aminium radical that promotes homolytic cleavage of the Si–B bond, releasing a silyl radical (see Scheme 3). After alkene addition, the resulting carbon radical is



Scheme 3. Dual Ir/Ni catalytic method described by Zhang and collaborators.

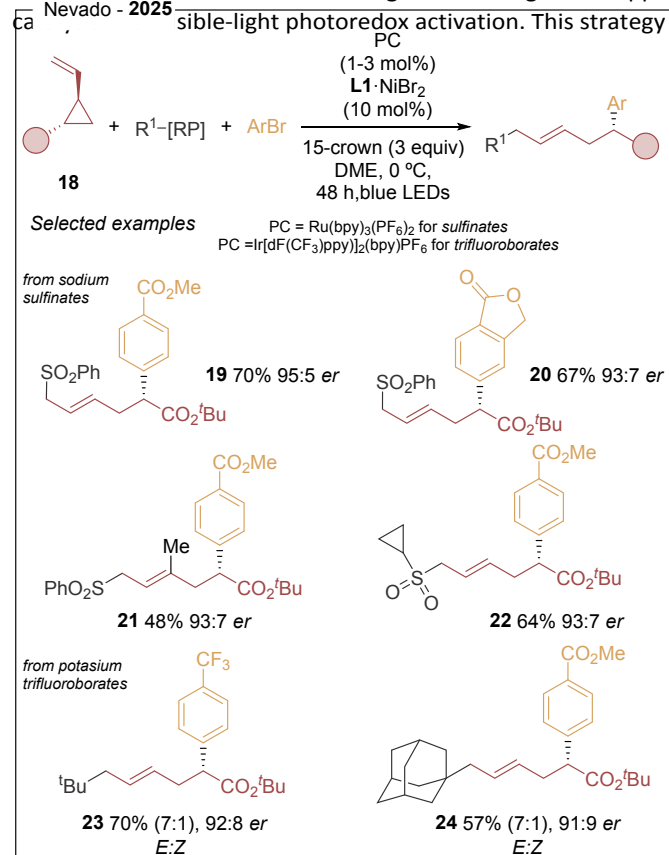
addition and reductive elimination to furnish the product (see Scheme 1).

Nevado reported in 2025 a versatile nickel/photoredox dual-catalysed asymmetric remote 1,5-carbosulfonylation and 1,5-dicarbonylation of vinyl cyclopropanes.¹³ This three-component strategy combines vinyl cyclopropanes **18** with sodium benzenesulfinate (or alkyl trifluoroborates) and aryl halides to access enantioenriched 1,5-difunctionalized alkenes. The carbosulfonylation reactions employ $\text{Ru}(\text{bpy})_3(\text{PF}_6)_2$ as photocatalyst in combination with NiBr_2 and hindered ligand **L1** (see Scheme 2). The method afforded 35 examples with excellent enantioselectivities and moderate to high yields (Scheme 4). In contrast, the 1,5-dicarbonylation process was optimally achieved from alkyl trifluoroborates using $\text{Ir}[\text{dF}(\text{CF}_3)\text{ppy}]_2(\text{bpy})\text{PF}_6$ and a $\text{NiCl}_2\cdot\text{py}$ complex, yielding 20 products with outstanding stereocontrol. Both protocols display broad substrate scope (**19–24**), high functional-group tolerance and remarkable synthetic utility, as demonstrated by late-stage functionalization of complex molecules. Mechanistically, the excited PC enables single-electron oxidation of the corresponding sulfinate or alkyl trifluoroborate, generating the corresponding sulfur- or carbon-centred radical. Addition of this species to the vinyl cyclopropane produces a secondary alkyl radical that undergoes fast ring opening to form a distal carbon-centred radical. This intermediate is intercepted by the chiral L^*Ni^0 complex following the general nickel cycle depicted in Scheme 1.

Dual copper/photoredox catalytic system

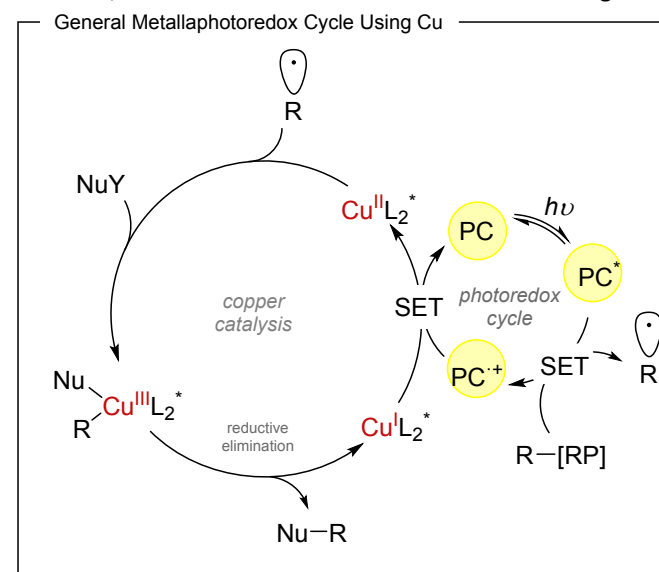
The low toxicity of copper along with its high natural abundance, makes this metal particularly attractive for catalytic

applications in organic synthesis.¹⁴ In addition, the well-established ability of copper complexes to efficiently intercept radical intermediates has encouraged the merger of copper



Scheme 4. Nickel/photoredox asymmetric remote 1,5-carbosulfonylation and 1,5-dicarbonylation of vinyl cyclopropanes.

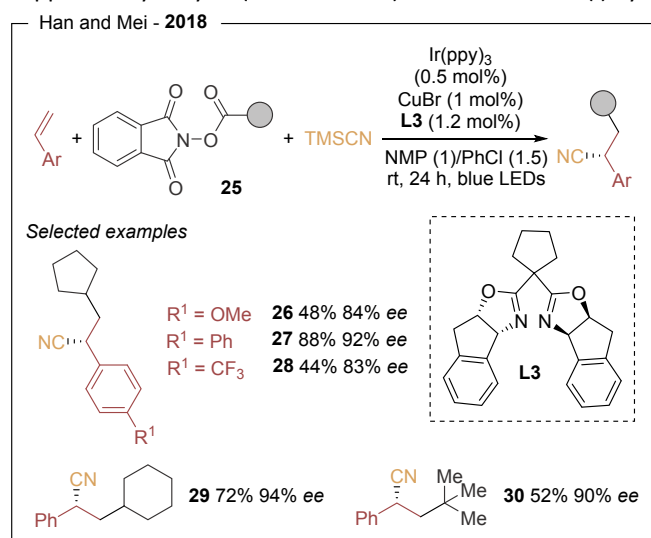
relies on two interconnected catalytic cycles, a photoredox cycle and a copper-mediated cross-coupling cycle. In the representative asymmetric transformations discussed in this review, photoexcitation of the PC species generates the excited state PC^* , which reduces a redox-active substrate through a



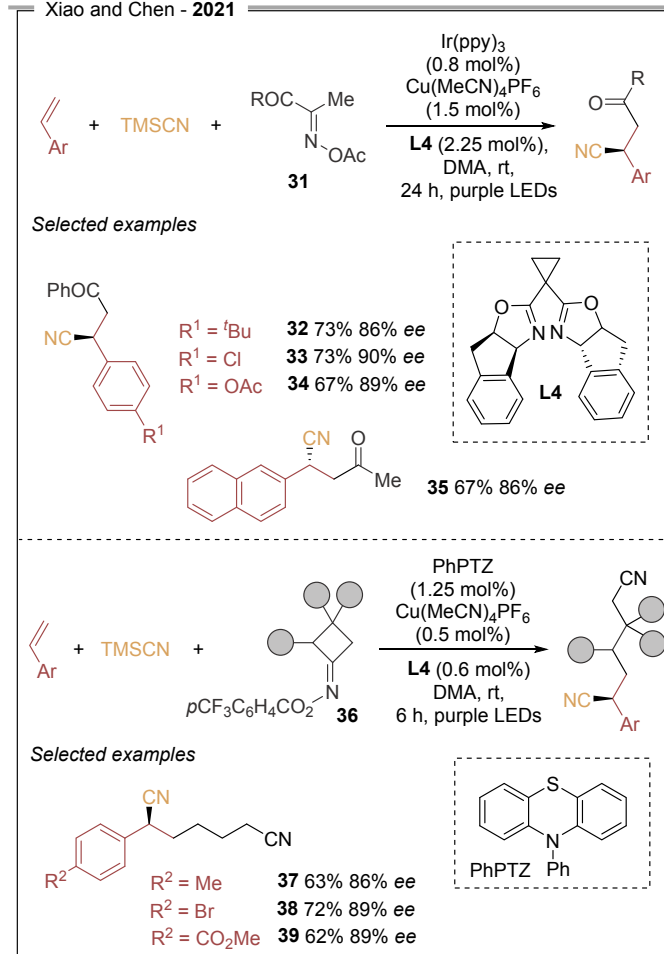
Scheme 5. General mechanism for photoredox/Cu dual catalysis processes.

single-electron transfer (SET) event (oxidative quenching), affording the oxidized form of the photocatalyst. A common mechanistic feature is the operation of a Cu^I/Cu^{II}/Cu^{III} manifold. In particular, high-valent chiral L*(alkyl)Cu(III)(X)₂ intermediates are generally proposed as the key species responsible for C–C or C–X bond formation. These complexes undergo facile reductive elimination to deliver the enantioenriched products in a stereocontrolled fashion (Scheme 5). Particularly, the enantioinduction is also mainly achieved through a C₂-symmetric chiral ligand that remain coordinated to copper throughout the catalytic cycle, with bis(oxazoline) derivatives consistently providing the best results.

In 2018, Han and Mei¹⁵ reported the first visible-light-induced asymmetric cyanoalkylation of alkenes, enabling the simultaneous formation of two C–C bonds in a three-component process. This transformation employs styrenes, redox-active esters (**25**) and TMS-CN as the cyanide source. The reaction proceeds efficiently under the combined action of Ir(ppy)₃, CuBr and a chiral bis(oxazoline) ligand (**L3**). Under the optimized conditions (Scheme 6), a wide range of styrenes reacted with the cyclopentyl redox active ester, identified as the most effective radical precursor. Both electron-donating and electron-withdrawing substituents were well tolerated at the *para* position of the aromatic ring (33–88% yield, 58–92% ee), while *meta*- and *ortho*-substituted derivatives also afforded the desired products in moderate to good yields and enantioselectivities (48–72% yield, 76–94% ee). The methodology proved general for different NHPI-derived alkyl fragments: primary alkyl esters such as methyl, ethyl and propyl provided high enantioselectivities (84–88% ee), and more sterically demanding groups, including isopropyl, cyclobutyl and tert-butyl, were also successfully incorporated (**26–30**). Mechanistically, single-electron reduction of the redox-active ester by Ir generates a radical anion and Ir^{IV}. Decarboxylation furnishes the corresponding alkyl radical, which adds to the styrene forming a stabilized benzylic radical that enters the copper catalytic cycle (see Scheme 5). Oxidation of LCu(I) by Ir^{IV}



Scheme 6. Cyanoalkylation method described by Han and Mei



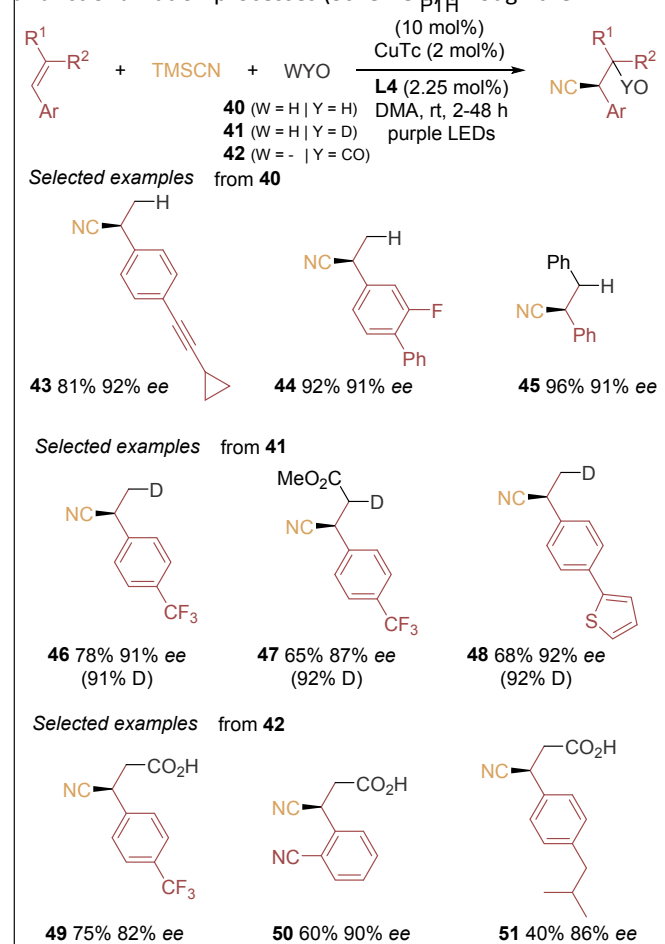
Scheme 7. Xiao and Chen's method to access enantioenriched β-cyanocarboxyls.

produces LCu^{II}, which captures the benzylic radical and coordinates TMS-CN to form an L(alkyl)(CN)Cu(III) intermediate. In 2021, Xiao and Chen¹⁶ reported an enantioselective three-component radical process that enables the stereocontrolled installation of two carbon fragments across alkenes, providing access to optically active β-cyano ketones and alkyl dinitriles. The transformation relies on the coupling of alkenes with oxime esters (**31** and **36**) as redox-active acyl radical precursors and TMS-CN under photoredox/copper dual catalysis using **L4** (Scheme 7). A broad range of alkenes proved to be compatible, including styrene derivatives (**32–35**, **37–39**) bearing both electron-donating and electron-withdrawing substituents. *Para*-substituted substrates afforded the desired products in 64–79% yield and 86–90% ee, while *meta*- and *ortho*-substituted styrenes delivered comparable results (61–81% yield, 86–93% ee). The method also displayed a wide oxime ester substrate scope, including aryl-, alkyl- and cycloketone-derivatives. Mechanistic studies suggest an oxidative-quenching photoredox cycle, in which SET reduction of the oxime ester generates an iminyl radical and a carboxylate anion. Subsequent C–C bond cleavage produces an acyl radical, which



adds to the alkene to form a stabilized benzylic radical, following a similar copper-mediated cycle as Han and Mei.

The same group further expanded the reactivity of 1,2-difunctionalized styrenes (Scheme 8) through the

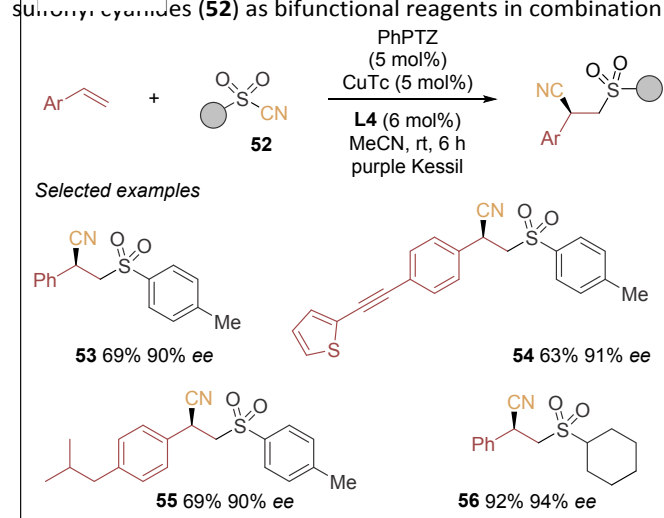


Scheme 8. Enantioselective cyanofunctionalization of styrenes.

enantioselective cyanofunctionalization of styrenes (hydrocyanation (**40**), deuterocyanation (**41**), and cyanocarboxylation (**42**)).¹⁷ For hydrocyanation and deuterocyanation protocols, styrene derivatives bearing *para*-sp² and sp substituents proved to be efficient substrates, providing 44 examples with enantioselectivities of up to 92% ee (**43-48**). Internal and conjugated alkenes were also well tolerated (29 examples, 48–96% yields and 64–92% ee). For the cyanocarboxylation reaction, a broad range of styrene derivatives containing both electron-donating and electron-withdrawing substituents on the aromatic ring afforded the corresponding chiral products in high enantioselectivities (**49-51**). On the basis of mechanistic studies, photoexcitation of the photocatalyst generates an alkene radical anion via SET, which reacts with an electrophilic partner (H₂O, D₂O, or CO₂) to form a benzylic radical that enters the copper catalytic cycle (see Scheme 5).

More recently, the same group¹⁸ reported access to a variety of enantioenriched β -sulfonyl nitriles through a visible-light-

induced, copper-catalyzed radical sulfonyl-cyanation of vinylarenes, enabling the simultaneous formation of C–C and C–S bonds across olefins (Scheme 9). This protocol employs sulfonyl cyanides (**52**) as bifunctional reagents in combination



Scheme 9. Copper-catalyzed radical sulfonyl-cyanation of styrenes.

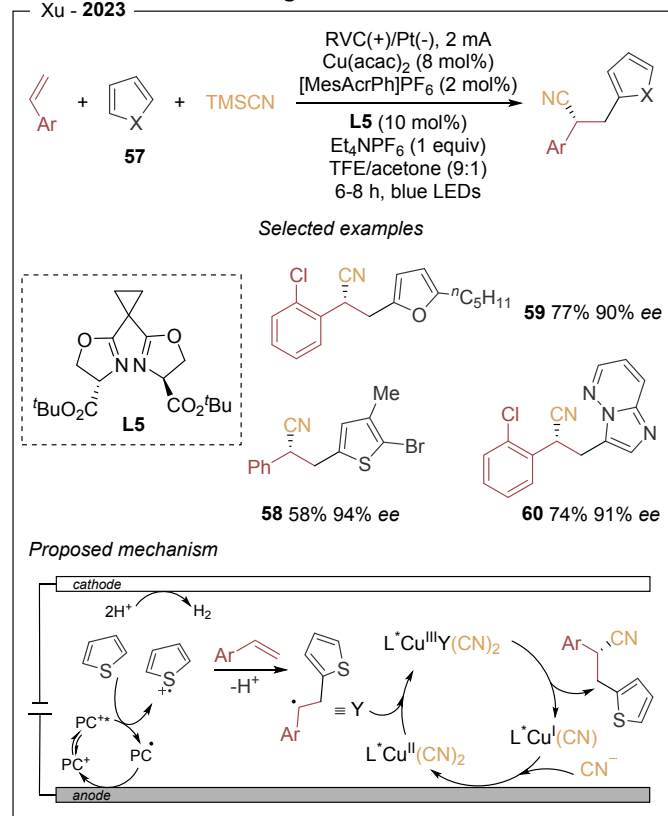
with styrenes, using PhPTZ (phenylphenothiazine) (see Scheme 7) as organic photocatalyst and a chiral copper complex generated from CuTc and Box **L4** (see Scheme 7) ligand. The generality of the method is demonstrated by the synthesis of 45 examples in yields and enantioselectivities of up to 98% and 95% ee, respectively (**53-56**). Notably, vinylarenes bearing extended π -systems, such as alkenyl and alkynyl groups at the *para*-position, performed well. The scope of the sulfonyl cyanide component includes alkyl-substituted derivatives bearing various functional groups along the carbon chain. Upon visible-light irradiation, PhPTZ* undergoes SET of the sulfonyl cyanide via an oxidative-quenching to generate a sulfonyl radical. This species rapidly adds to the styrene, forming a stabilized benzylic radical intermediate. Meanwhile, the chiral L*Cu(I)Tc complex is oxidized by the photocatalyst radical cation (PhPTZ⁺) through a SET process to afford an L*Cu^{II}(CN)(Ts) species. Capture of the benzylic radical led to the formation of the final product (see Scheme 5).

Lastly, Xu described an electrophotocatalyzed asymmetric heteroarylcyanation of aryl alkenes via C–H functionalization (Scheme 10).¹⁹ This three-component transformation involves styrenes, heteroarenes (**57**), and TMSCN, and employs an acridinium hexafluorophosphate as photocatalyst in combination with a chiral Box (**L6**) ligand–copper complex as the asymmetric catalytic system. The method enables the incorporation of a wide range of heteroarenes, including 2- and 3-substituted thiophenes, 2-pentylfurans, N-protected pyrroles, imidazobicycles, and 2,6-dimethoxypyridine. The method affords in general high yields and excellent enantioselectivities (up to 97% ee). Mechanistic investigations indicate that the excited acridinium state undergoes SET to the heteroarene to generate an arene radical cation together with the reduced acridine radical. Anodic oxidation then regenerates



the ground-state acridinium catalyst, closing the photoredox cycle. The electrophilic arene radical cation subsequently engages the alkene in a regioselective intermolecular addition

Xu - 2023



Scheme 10. Electrophotocatalyzed asymmetric heteroarylcyanation of aryl alkenes.

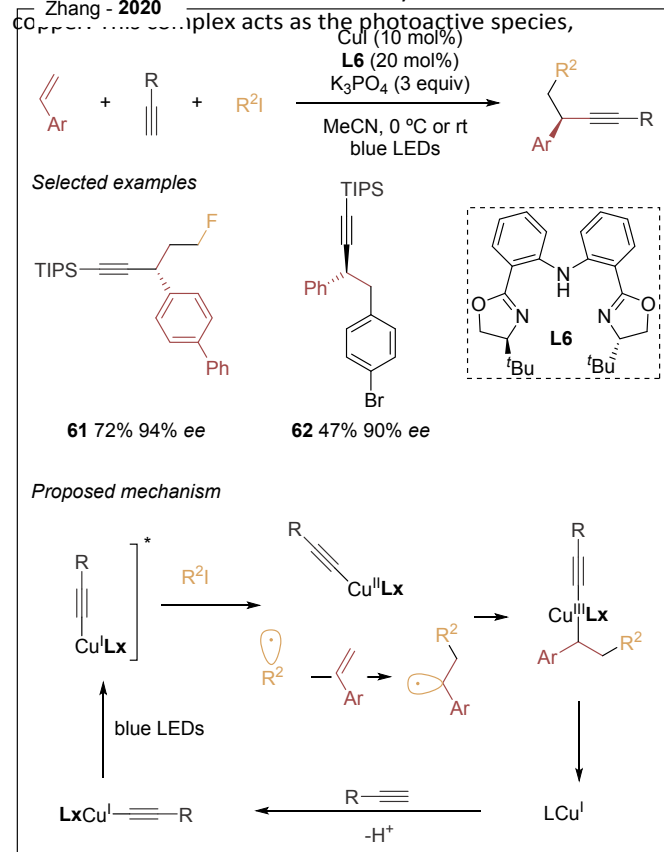
to form a distal radical cation intermediate, which after deprotonation furnishes a stabilized benzylic radical. This radical is intercepted by the chiral $\text{LCu}^{\text{II}}(\text{CN})_2$ complex to generate a high-valent $\text{L}(\text{alkyl})\text{Cu}^{\text{III}}(\text{CN})_2$ species. Reductive elimination from this Cu^{III} intermediate provides enantioenriched heteroarylcyanation product.

Copper as bifunctional catalyst

In 2020, Zhang²⁰ reported a photoinduced asymmetric copper-catalyzed dual alkylation/arylation and alkylation of alkenes. This three-component transformation couples (hetero)aryl alkenes, terminal alkynes, and alkyl or aryl iodides, providing access to a broad range of enantioenriched propargylic scaffolds in moderate to high yields and excellent enantioselectivities (Scheme 11). Notably, no external photocatalyst is required, and **L6** ligand proved optimal in terms of asymmetric induction. Both electron-donating and electron-withdrawing substituents were well tolerated at the para position of styrenes, whereas ortho-substituted derivatives afforded the desired products in lower yields but maintained excellent enantioselectivities (42–47% yield, 92–95% ee). Importantly, fluorinated haloalkanes were successfully incorporated, enabling access to propargylic compounds bearing CF_2 , CHF , $\text{CF}_2\text{CF}_2\text{H}$, and CF_2CF_3 motifs. On the basis of

mechanistic studies, the authors proposed that, in the presence of K_3PO_4 , a chiral $[\text{L}(\text{C}\equiv\text{CR})\text{Cu}(\text{I})]^-$ species is formed via deprotonation of the terminal alkyne and coordination to

Zhang - 2020



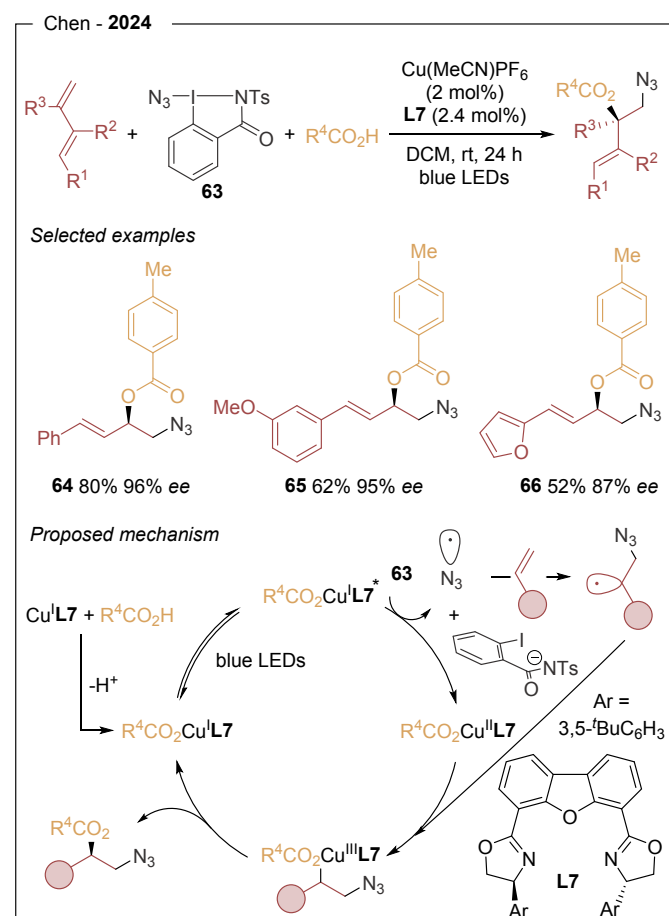
Scheme 11. Enantioselective dual carbofunctionalization of alkenes reported by Zhang.

undergoing excitation and transferring an electron to the alkyl iodide, thereby generating a Cu^{II} species and an alkyl radical. The latter adds to the styrene to form a stabilized benzylic radical, which is subsequently trapped by the Cu^{II} intermediate to furnish a Cu^{III} complex. Enantioselective reductive elimination then delivers the final product.

Chen's group²¹ reported in 2024 an asymmetric photoinduced copper-catalyzed three-component radical 1,2-azidoxygenation of 1,3-dienes using organic azide **63** and a palette of carboxylic acids (Scheme 12). Optimization of the chiral ligand identified **L7** as the optimal choice, likely due to the steric demand of its 1,3-bis(*tert*-butyl)phenyl substituents. This protocol displays broad substrate scope, high functional-group tolerance, and excellent control over chemo-, regio-, and enantioselectivity, providing access to azidated chiral allylic esters. Mechanistically, a photosensitive chiral $\text{L}(\text{O}_2\text{Car})\text{Cu}(\text{I})$ complex is formed via ligand exchange from $\text{Cu}(\text{MeCN})_4\text{PF}_6$. Upon irradiation with blue LEDs, this species reaches a strongly reducing excited state that undergoes SET with **63**, generating an azidyl radical and a Cu^{II} intermediate. The azidyl radical adds to the terminal alkene of the 1,3-diene to form an allylic radical, which is subsequently trapped by the Cu^{II} species to give a π -



allyl Cu(III) intermediate. Stereocontrolled reductive elimination from this species affords the final product.

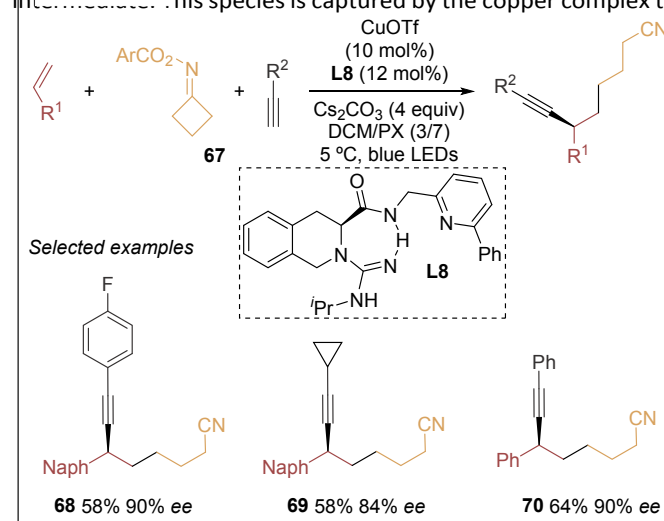


Scheme 12. Copper-catalyzed 1,2-azidoxygenation of 1,3-dienes.

Lastly, Liu²² described a photoinduced asymmetric cyanoalkylalkynylation of alkenes using cycloketone oxime esters and terminal alkynes as radical precursors, in combination with copper and a tridentate chiral ligand **L8** (Scheme 13). This protocol provides access to a range of enantioenriched alkyne–nitrile derivatives with good functional-group tolerance. Substituted ethynylbenzenes afforded moderate yields, while alkyl- and TMS-substituted alkynes, as well as 2-ethynyl-naphthalene and 3-ethynylthiophene, were also compatible. A variety of alkenes and cycloketone oxime esters were evaluated; notably, 6-substituted 2-vinylnaphthalenes bearing both electron-donating and electron-withdrawing groups performed well. Heteroaryl substrates, including benzothiophene, benzodioxole, N-tosylindole, and benzofuran derivatives, were also successfully incorporated, affording the corresponding products in 45–55% yield and 82–85% ee. However, other oxime substrates resulted in lower enantioselectivities.

A plausible mechanism involves initial formation of a copper(I) acetylide complex upon coordination of the terminal alkyne to the chiral ligand in the presence of base. Upon light irradiation,

this species reaches an excited state capable of reducing the oxime ester via SET, generating a Cu^{II} acetylide and an imino radical. Subsequent fragmentation affords a cyanoalkyl radical, which adds to the alkene to generate a carbon-centered radical in the presence of this species is captured by the copper complex to



Scheme 13. Copper-catalyzed 1,2-azidoxygenation of 1,3-dienes.

form a Cu^{III} intermediate, which undergoes reductive elimination to furnish the cyanoalkylalkynylation product while regenerating the Cu^I catalyst.

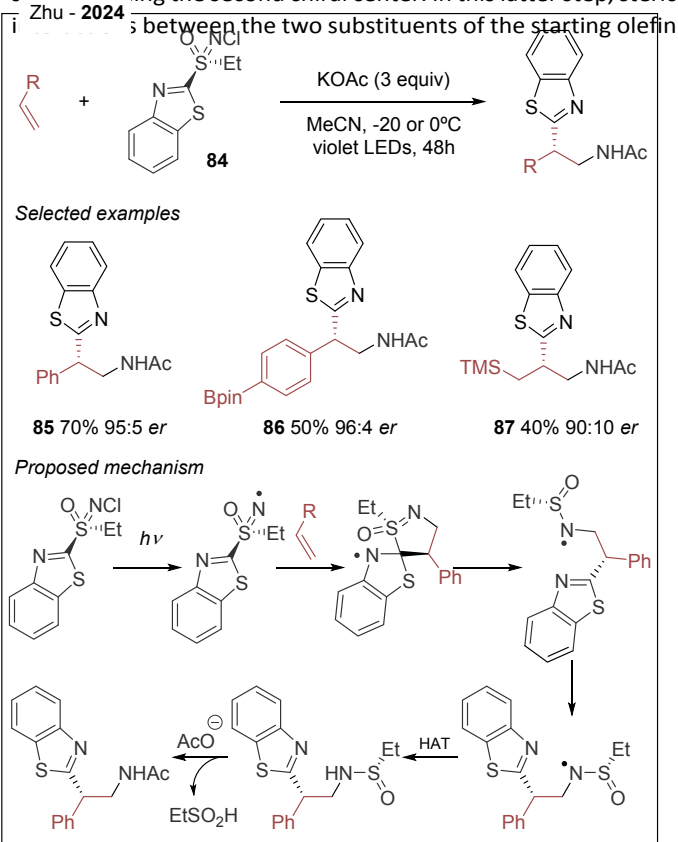
Dual chromium/photoredox catalytic system

Organochromium reagents emerged as powerful intermediates in the late 1970s with the development of the Nozaki–Hiyama–Kishi reaction for the allylation of aldehydes, which has been widely applied in the synthesis of natural products.²³ Subsequently, chemists sought to exploit photocatalysis and electrocatalysis as complementary strategies to generate organochromium^{III} species. In this context, the merger of chromium catalysis with photoredox activation was first reported by the Glorius group in 2018.^{9b,24}

In 2022, Wang²⁵ reported an asymmetric three-component 1,4-functionalization of 1,3-enynes to access chiral allenols through the merger of photoredox and chromium catalysis (Scheme 14). This transformation combines aldehydes (**71**), 1,3-enynes (**72**), and DHP esters (**73**), using 4CzIPN as the photocatalyst in combination with CrCl₂ and a chiral cyano-bisoxazoline ligand **L9**. The protocol exhibits excellent regioselectivity and enables simultaneous control of axial and central chirality. A broad range of aromatic and aliphatic aldehydes (52 examples) afforded the desired products in high to excellent yields (up to 95%), with diastereomeric ratios of up to 20:1 and enantioselectivities of up to 96% ee (**74–76**). Based on mechanistic experiments and precedents, the authors proposed that the excited photocatalyst undergoes SET with the DHP ester, generating the reduced photocatalyst and the radical cation of the DHP species. Fragmentation of this radical cation produces an alkyl radical and a substituted pyridinium



(arylsulfinyl)amide adds to the cationic species generating a new C-N bond and the first stereogenic center dictated by the chiral sulfinyl moiety. The resulting benzylic radical intermediate undergoes 1,4-aryl shift via a spirocyclic transition state affording the second chiral center. In this latter step, steric



Scheme 16. General mechanism for the photoredox/Cu dual catalysis processes.

are responsible for the preferential aryl translocation. The catalytic cycle closes after SET from the Ir^{II} species, triggering N-S bond fragmentation and affording the final product. In sharp contrast, when electron-poor alkenes such as vinylamides are used, the first SET step with the photocatalyst is thermodynamically unfavorable and the single-electron oxidation of the deprotonated N-(arylsulfinyl)amide to form a N-centered radical seems to be the preferred pathway (Scheme 15, bottom right). This radical adds to the olefin, point in which the two mechanistic pathways converge.

A complementary asymmetric aminoheteroarylation of alkenes has been reported by Zhu exploiting the light-sensitivity of chiral sulfoximines (Scheme 16).²⁹ In this approach, no external photocatalyst is required, but the sulfoximine reagent **84** undergoes direct homolysis of the N-Cl bond under irradiation of LED light ($\lambda_{em} = 425$ nm), generating a key N-centered radical which rapidly adds to the olefin. These two steps are supported by radical trapping experiments using TEMPO, which confirmed the formation of adduct derived from the benzylic radical intermediate species (Scheme 16). Although the reported yields are moderate the method produces *er* up to 97:3 and

represents a useful transition metal free alternative to the formation of enantioenriched heteroarylethylacetamides, operating under mild conditions.

Conclusions

Over the last few years, visible-light photochemistry has transformed the landscape of asymmetric alkene difunctionalization. The precise stereochemical control of open-shell intermediates has evolved into a powerful and versatile synthetic strategy for alkene difunctionalization reactions. The convergence of photoredox catalysis with transition-metal catalysis, hydrogen-bonding organocatalysis, and chiral reagent design has demonstrated that radical chemistry can be both sustainable and highly enantioselective. Metallaphotoredox dual catalysis has emerged as a particularly robust platform, enabling efficient interception of photogenerated radicals by nickel, copper, or chromium complexes to deliver well defined C-C and C-X bonds. In parallel, cooperative hydrogen-bonding strategies have shown that purely noncovalent interactions can orchestrate demanding radical additions and even radical-radical couplings with remarkable enantioselectivity. Despite the impressive progress achieved, challenges remain in expanding substrate scope to less activated alkenes, improving predictability of stereochemical models, and enhancing scalability and efficiency. Nevertheless, the advances summarized in this review clearly establish light-mediated asymmetric alkene difunctionalization as a mature and rapidly growing domain of modern synthesis.

Author contributions

All authors have given approval to the final version of the manuscript.

Conflicts of interest

There are no conflicts to declare.

Data availability

No primary research results, software or code have been included and no new data were generated or analyzed as part of this review.

Acknowledgements

Support for this work under grants PID2024-156087NB-I00, RED2022-134287-T, and 2021SGR00064 from AGAUR Generalitat de Catalunya are gratefully acknowledged.

Notes and references

- H. Jiang and A. Studer, *Chem. Soc. Rev.*, 2020, **49**, 1790–1811.
- a) Y. Wang, Z.-P. Bao, X.-D. Mao, M. Hou and X.-F. Wu, *Chem. Soc. Rev.*, 2025, **54**, 9530–9573. b) R. K. Dhungana, S. Kc, P.



- Basnet and R. Giri, *Chem. Rec.*, 2018, **18**, 1314–1340. c) B. Shrestha, P. Basnet, R. K. Dhungana, S. Kc, S. Thapa, J. M. Sears and R. Giri, *J. Am. Chem. Soc.*, 2017, **139**, 10653–10656.
- 3 a) M. J. Cabrera-Afonso, A. Sookezian, S. O. Badir, M. El Khatib and G. A. Molander, *Chem. Sci.*, 2021, **12**, 9189–9195. b) P. Sarró, Y. Ji, A. Gallego-Gamo, C. Gimbert-Suriñach, A. Vallribera and A. Granados, *Org. Chem. Front.*, 2025, **12**, 3475–3492. c) A. Gallego-Gamo, P. Sarró, Y. Ji, C. Gimbert-Suriñach, A. Vallribera and A. Granados, *J. Org. Chem.*, 2024, **89**, 4776–4787. d) A. Granados, R. K. Dhungana, M. Sharique, J. Majhi and G. A. Molander, *Org. Lett.*, 2022, **24**, 4750–4755. e) P. Sarró, A. Gallego-Gamo, E. Molins, R. Pleixats, C. Gimbert-Suriñach, A. Vallribera, A. Granados, *Org. Lett.*, 2025, **27**, 11372–11377. f) Y. Ji, A. Jaafar, C. Gimbert-Suriñach, M. Ribagorda, A. Vallribera, A. Granados and M. J. Cabrera-Afonso, *Org. Chem. Front.*, 2024, **11**, 6660–6665.
- 4 a) T. Yang, W. Xiong, G. Sun, W. Yang, M. Lu and M. J. Koh, *J. Am. Chem. Soc.*, 2024, **146**, 29177–29188. b) X. Li, M. Yuan, F. Chen, Z. Huang, F.-L. Qing, O. Gutierrez and L. Chu, *Chem*, 2023, **9**, 154–169. c) X. Wei, W. Shu, A. García-Domínguez, E. Merino and C. Nevado, *J. Am. Chem. Soc.*, 2020, **142**, 13515–13522. d) X. Hu, I. Cheng-Sánchez, W. Kong, G. A. Molander and C. Nevado, *Nat. Catal.*, 2024, **7**, 655–665.
- 5 a) M. H. Shaw, J. Twilton and D. W. C. MacMillan, *J. Org. Chem.*, 2016, **81**, 6898–6926. b) N. A. Romero and D. A. Nicewicz, *Chem. Rev.*, 2016, **116**, 10075–10166.
- 6 H.-T. Zhao, J.-N. Lin, W. Shu, *Chem. Eur. J.*, 2024, **30**, e202402712.
- 7 Z.-L. Zhou, Y. Zhang, P.-Z. Cui and J.-H. Li, *Chem.-Eur. J.*, 2024, **30**, e202402458.
- 8 a) Y. Liu, H. Liu, X. Liu, Z. Chen, *Catalysts*, 2023, **13**, 1056. b) S. Mondal, S. Ghosh, A. Hajra, *Chem. Commun.*, 2024, **60**, 9659–9691.
- 9 a) J. C. Tellis, C. B. Kelly, D. N. Primer, M. Jouffroy, N. R. Patel, G. A. Molander, G. A. *Acc. Chem. Res.*, 2016, **49**, 1429–1439. b) A. Y. Chan, I. B. Perry, N. B. Bissonnette, B. F. Buksh, G. A. Edwards, L. I. Frye, O. L. Garry, M. N. Lavagnino, B. X. Li, Y. Liang, E. Mao, A. Millet, J. V. Oakley, N. L. Reed, H. A. Sakai, C. P. Seath and D. W. C. MacMillan, *Chem. Rev.*, 2022, **122**, 1485–1542.
- 10 a) S. O. Badir, G. A. Molander, *Chem*, 2020, **6**, 1327–1339. b) F. Manzoor, A. Majeed, A. H. Ibrahim, M. A. Iqbal, A. Rehman, S. Aziz, A. Shahzadi, S. Fatima, S. Ejaz, M. S. Zafar, *RSC Adv.*, 2025, **15**, 33345–33364.
- 11 X. Du, I. Cheng-Sánchez, C. Nevado, *J. Am. Chem. Soc.*, 2023, **145**, 12532–12540.
- 12 Q. Yuan, Z. Deng, Y. Wan, Y. Zhang, *Org. Lett.*, 2025, **27**, 680–685.
- 13 X. Du, M. E. Lennon, G. Kriticou, C. Nevado, *Nat. Commun.*, 2025, **16**, 6958.
- 14 a) J. Sobieski, A. Gorcynski, A. M. Jazani, G. Yilmaz, K. Matyjaszewski, *Angew. Chem. Int. Ed.* 2025, **64**, e202415785. b) N. Chakraborty, D. Barik, B. Das, B. K. Patel, *Chem. Asian J.*, 2025, **20**, e00692.
- 15 W. Sha, L. Deng, S. Ni, H. Mei, J. Han, Y. Pan, *ACS Catal.*, 2018, **8**, 7489–7494
- 16 P.-Z. Wang, Y. Gao, J. Chen, X.-D. Huan, W.-J. Xiao, J.-R. Chen, *Nat. Commun.*, 2021, **12**, 1815.
- 17 B. Zhang, T.-T. Li, Z.-C. Mao, M. Jiang, Z. Zhang, K. Zhao, W.-Y. Qu, W.-J. Xiao, J.-R. Chen, *J. Am. Chem. Soc.*, 2024, **146**, 1410–1422.
- 18 K. Zhao, B. Zhang, F.-Y. Zhao, W.-J. Xiao, J.-R. Chen, *ChemCatChem*, 2025, **17**, e202500258.
- 19 X.-L. Lai, H.-C. Xu, *J. Am. Chem. Soc.*, 2023, **145**, 18753–18759.
- 20 Y. Zhang, Y. Sun, B. Chen, M. Xu, C. Li, D. Zhang, G. Zhang, *Org. Lett.* 2020, **22**, 1490–1494.
- 21 G.-Q. Li, Z.-Q. Li, M. Jiang, Z. Zhang, Y. Qian, W.-J. Xiao, J.-R. Chen, *Angew. Chem. Int. Ed.* 2024, **63**, e202405560.
- 22 S. Xin, J. Liao, Q. Tang, X. Feng, X. Liu, *Chem. Sci.*, 2024, **15**, 18557–18563. View Article Online
DOI: 10.1039/D6OB00441E
- 23 A. Gil, F. Albericio, M. Álvarez, *Chem. Rev.*, 2017, **117**, 8420–8446.
- 24 J. L. Schwarz, F. Schäfers, A. Tlahuext-Aca, L. Lückemeier, F. Glorius, *J. Am. Chem. Soc.* 2018, **140**, 12705–12709.
- 25 F.-H. Zhang, X. Guo, X. Zeng, Z. Wang, *Nat. Commun.*, 2022, **13**, 5036.
- 26 T. M. Monos, R. C. McAtee, C. R. J. Stephenson, *Science*, 2018, **361**, 1369–1373.
- 27 E. A. Noten, C. H. Ng, R. M. Wolessensky, C. R. J. Stephenson, *Nat. Chem.*, 2024, **16**, 599–606.
- 28 C. Hervieu, M. S. Kirillova, Y. Hu, S. Cuesta-Galisteo, E. Merino, C. Nevado, *Nat. Chem.*, 2024, **16**, 607–614.
- 29 Z. Cao, Y. Sun, Y. Chen, C. Zhu, *Angew. Chem. Int. Ed.*, 2024, **63**, e202408177.



No primary research results, software or code have been included and no new data were generated or analysed as part of this review.

View Article Online
DOI: 10.1039/D6OB00441E

